Polymer stabilization of electrohydrodynamic instability in non-iridescent cholesteric thin films

Yu-Cheng Hsiao and Wei Lee*

Institute of Imaging and Biomedical Photonics, College of Photonics, National Chiao Tung University, Guiren Dist., Tainan 71150, Taiwan

*wlee@nctu.edu.tw

Abstract: A non-iridescent cholesterol liquid crystal (CLC) thin film is demonstrated by using the polymer-stabilized electrohydrodymanic (PSEHD) method. The photopolymerized cell made from a CLC/monomer mixture exhibits an optically stable gridlike pattern. The helical axis of thus-formed CLC is aligned with the hydrodynamic flow induced by a space charge motion, and the arrayed CLC grid configuration renders a wide viewing angle thanks to the limited color shift at various lines of sight. The formation of the PSEHD structure was verified with polarized optical microscopy, ascertaining that the electrohydrodymanic pattern can be photo-cured or stabilized. The PSEHD CLC is simple to fabricate and potentially suitable for applications in wide-viewing-angle or non-iridescent devices.

OCIS codes: (160.3710) Liquid crystals; (160.1585) Chiral media; (160.4890) Organic materials; (230.3720) Liquid-crystal devices.

References and links

1. D.-K. Yang, J. L. West, L. C. Chien, and J. W. Doane, "Control of reflectivity and bistability in displays using cholesteric liquid crystals," J. Appl. Phys. **76**(2), 1331–1333 (1994).
2. D.-K. Yang, J. W. Doane, Z. Yaniv, and J. Glasser, "Cholesteric reflective display: Drive scheme and contrast," Appl. Phys. Lett. **64**(15), 1905–1907 (1994).
3. S.-T. Wu and D.-K. Yang, *Reflective Liquid Crystal Displays* (Wiley, 2001), Ch. 8.
4. Y.-C. Hsiao, C.-Y. Wu, C.-H. Chen, V. Ya. Zyryanov, and W. Lee, "Electro-optical device based on photonic structure with a dual-frequency cholesteric liquid crystal," Opt. Lett. **36**(14), 2632–2634 (2011).
5. Y.-C. Hsiao, C.-T. Hou, V. Ya. Zyryanov, and W. Lee, "Multichannel photonic devices based on tristable polymer-stabilized cholesteric textures," Opt. Express **19**(24), 23952–23957 (2011).
6. Y.-C. Hsiao, Y.-H. Zou, I. V. Timofeev, V. Ya. Zyryanov, and W. Lee, "Spectral modulation of a bistable liquid-crystal photonic structure by the polarization effect," Opt. Mater. Express **3**(6), 821–828 (2013).
7. Y.-T. Lin and T.-H. Lin, "Cholesteric liquid crystal display with wide viewing angle based on multi-domain phase-separated composite films," J. Disp. Technol. **7**(7), 373–376 (2011).
8. D.-K. Yang, J. L. West, L.-C. Chien, and J. W. Doane, "Control of reflectivity and bistability in displays using cholesteric liquid crystals," J. Appl. Phys. **76**(2), 1331–1333 (1994).
9. D.-K. Yang, Z. Lu, and J. W. Doane, "Bistable polymer dispersed cholesteric liquid crystal displays," United States Patent 6061107A. (May 9, 2000).
10. D.-K. Yang, "Flexible bistable cholesteric reflective displays," J. Disp. Technol. **2**(1), 32–37 (2006).
11. Y.-C. Hsiao and W. Lee, "Lower operation voltage in dual-frequency cholesteric liquid crystals based on the thermodielectric effect," Opt. Express **21**(20), 23927–23933 (2013).
12. Y.-C. Hsiao, C. Y. Tang, and W. Lee, "Fast-switching bistable cholesteric intensity modulator," Opt. Express **19**(10), 9744–9749 (2011).
13. Y.-C. Hsiao, H.-T. Wang, and W. Lee, "Thermodielectric generation of defect modes in a photonic liquid crystal," Opt. Express **22**(3), 3593–3599 (2014).
14. I. P. Ilchishin, L. N. Lisetski, and T. V. Mykytiuk, "Reversible phototuning of lasing frequency in dye doped cholesteric liquid crystal and ways to improve it," Opt. Mater. Express **1**(8), 1484–1493 (2011).
15. L. Kramer and W. Pesch, "Convection instabilities in nematic liquid crystals," Annu. Rev. Fluid Mech. **27**(1), 515–539 (1995).
16. S. Kai and W. Zimmermann, "Pattern dynamics in the electrohydrodynamics of nematic liquid crystals," Prog. Theor. Phys. Suppl. **99**, 458–492 (1989).
17. W. Helfrich, "Conduction-induced alignment of nematic liquid crystals: basic model and stability considerations," J. Chem. Phys. **51**(9), 4092–4105 (1969).
18. E. F. Carr, "Influence of electric fields on the molecular alignment in the liquid crystal p-(anisalamino)-phenyl acetate," Mol. Cryst. Liq. Cryst. (Phila. Pa.) **7**, 253–268 (1969).

#243823 Received 25 Jun 2015; revised 6 Aug 2015; accepted 11 Aug 2015; published 19 Aug 2015

19. J. H. Huh, "Electrohydrodynamic instability in cholesteric liquid crystals in the presence of a magnetic field," Mol. Cryst. Liq. Cryst. (Phila. Pa.) **477**, 67–76 (2007).
20. W. Helfrich, "Electrohydrodynamic and dielectric instabilities of cholesteric liquid crystals," J. Chem. Phys. **55**(2), 839–842 (1971).
21. J. P. Hurault, "Static distortions of a cholesteric planar structure induced by magnetic or ac electric fields," J. Chem. Phys. **59**(4), 2068–2075 (1973).
22. D.-K. Yang, X.-Y. Huang, and Y.-M. Zhu, "Bistable cholesteric reflective displays: Materials and drive schemes," Annu. Rev. Mater. Sci. **27**(1), 117–146 (1997).
23. M. Lu and H. Yuan, "Bistable cholesteric liquid crystal displays with very high contrast and excellent mechanical stability," United States Patent 5570216A (October 29, 1996).

1. Introduction

Cholesteric liquid crystals (CLCs) are intriguing optical materials that possess unique physical and mechanical properties such as dielectric anisotropy, birefringence, optical bistability, Bragg reflection, and flexibility for photonic device applications. Based on these features, CLCs have been suggested for use in reflective CLC displays [1–3] and many other optoelectronic applications [4–6]. Because the reflective and bistable nature of CLC displays requires power only needed to update a frame or an image, these CLC devices are characterized by the advantage of low power consumption [7]. The bistable properties of CLC displays have been well documented by Yang *et al*. By employing surface treatments or adding polymeric components, they have realized bistable CLC displays and made them flexible [8–10]. Unfortunately, CLCs have some unavoidable problems such as high operation voltage and slow response speed. There are a good number of efforts aiming to solve the problems concerning high operation voltage and slow electro-optical response in CLCs [11,12]. As a matter of fact, CLCs for photonic applications generally suffer from another limitation—the iridescence or narrow viewing angle. CLCs with a pitch length comparable to the optical wavelength (in the planar state) can be regarded as one-dimensional photonic crystals [13, 14]. The left-handed circularly polarized light is reflected when linearly polarized light propagates into a left-handed CLC cell along the helical axis. The reflected wavelength λ follows the relationship $\lambda = n{\cdot}P \cos\theta$, where n is the average refractive index of the LC, P is the pitch length of the helix, and θ is the angle of light incidence. Accordingly, the reflective color as viewed is strongly dependent of the viewing angle. The reflection bandwidth $\Delta\lambda$ satisfies the equation: $\Delta\lambda = \Delta n{\cdot}P \cos\theta$, where the birefringence or optical anisotropy $\Delta n = n_e - n_o$ and $\Delta\lambda$ again depends strongly on the angle of incidence [7]. Obviously, the incident-angle-dependent Bragg reflection makes pristine CLCs iridescent and, thus, unsuitable for use in displays that require a wide viewing angle.

An AC-driven electrohydrodynamic (EHD) convection instability that occurs in nematic LCs has been extensively studied in detail over the past half century [15,16]. This instability gives rise to a rich variety of stationary and nonstationary EHD patterns. The most well-known pattern is called the Williams domain induced by the Carr–Helfrich instability [17,18]. Other various EHD patterns can take place as well on the basis of the initial distribution of the director field, where the director stands for a vector that defines a locally averaged orientation of the LC molecules. In CLCs, however, the pitch itself serves as a critical part in understanding the EHD instability and the resulting pattern formation [19]. Typical to CLCs is a gridlike pattern (GP) even though CLCs exhibit a few distinct patterns contingent on the pitch length [20,21]. These effects are connected with EHD convection owing to the anisotropies of the dielectric constant and conductivity in the mesogenic materials. The GP can be observed as long as the externally applied field retains. In other words, a CLC relaxes to its former orientation (i.e., the Grandjean planar texture) once the applied voltage is turned off. In contrast to the EHD observations mentioned above, the CLC fabricated in this work contains a rather small amount of photo-curable prepolymer. This novel approach permits the stabilization of the GP (and other EHD instability patterns in general) by means of photopolymerization of the multicomponent precursor, thereby minimizing color shift for a non-iridescent structure.

#243823 Received 25 Jun 2015; revised 6 Aug 2015; accepted 11 Aug 2015; published 19 Aug 2015

2. Experiment

The CLC material used in this experiment is a blend of a nematic LC (HEF951800-100, HCCH) and a chiral dopant (S811, Merck) at a concentration of 20 wt%. In order to form polymer network in the later stage of sample fabrication to attain a stabilized EHD pattern in the cell, the following agents were added into the CLC material in preparation of a suitable CLC/monomer mixture: the reactive mesogen RM257 (Merck) at 5 wt%, the trifunctional monomer trimethylolpropane triacrylate (TMPTA, Sigma–Aldrich) at 3 wt%, and the photoinitiator Irgacure 184 (BASF) at 1 wt%. The homogenized mixture was introduced into empty cells of 11 μm in gap by capillary action. (The inner surfaces of the cell substrates were pre-coated with transparent indium–tin oxide prior to assembly.) Polyimide (Nissan SE-8793), the alignment agent, was employed in the cells and rubbed in antiparallel to impose the initial planar state for both CLCs and polymer-stabilized (PS) counterparts. Each filled cell was then photopolymerized with ultraviolet (UV) light at wavelengths of 350–380 nm and intensity of 2 mW/cm^2 for 30 s. Note that the UV exposure was performed when an AC voltage (at the threshold voltage) was simultaneously applied across the cell thickness to allow the LC director to lie in the plane of space charge flow. Figure 1 schematically depicts the polymer-stabilized EHD (PSEHD) CLC structure. The formation of the PSEHD configuration (namely, GP) is the result of uniform UV illumination that generates polymer network and, in turn, stabilizes the GP pattern in the mesogenic bulk. Because of the polymer stabilization, the pattern is preserved or stable after the voltage is removed. The transmission spectra of the LC cells were acquired with a high-resolution fiber-optic spectrometer (Ocean Optics HR2000 +). A conventional planar-alignment pristine CLC cell was also prepared as a reference for the study of the effect of PSEHD GP on the viewing angle. An arbitrary function generator (Tektronix AFG-3022B) was used to supply various frequency-modulated sinusoidal-wave for bistable switching between the planar and focal conic states in a PSEHD GP cell. All experimental data were measured at an ambient temperature of 26 ± 1 °C.

3. Results and discussion

We applied an AC voltage (at a frequency f = 1 Hz–1 MHz) to induce GPs. At a higher chiral-dopant concentration, the GP is the only type of EHD patterns that can be generated in CLCs. To observe the PSEHD effect, the PSCLC cells were examined under a polarized optical microscope (POM). Figure 2(a) comparatively presents a POM image of a typical EHD GP as reported in the literature, whereas Fig. 2(b) shows an exemplary PSEHD GP observed in our PSCLCs. For this specific case where the images were taken, the EHD GP was formed in a CLC cell consisting of all of the necessary constituents for the subsequent fabrication of a PSCLC. That is to say, Figs. 2(a) and 2(b) are associated with the same cell before and after photopolymerization, respectively. The "polymerization of the EHD structure" does not affect the morphology of the GP. The periodic, two-dimensional (2-D) GP reflects the characteristic of the CLC's helical pitch. It is clearly different from the Williams domain patterns observed in NLCs, and the GP can be observed in CLCs with a sufficiently small pitch. Yang *et al.* proposed the use of SiO_2 alignment layers to widen the viewing angle in CLCs. However, random domain sizes resulted—similar to the optically scattering focal conic state—and many defects were exhibited in thus-made cells [22]. In comparison, our PSEHD cell shows a 2-D, periodic-array pattern in imperfect but ordered (i.e., gridlike) planar texture. Accordingly, it is more suitable and reliable for CLC devices. Figure 3 delineates the frequency-dependent threshold voltage required to induce the EHD GP. The data of the threshold voltage can be used as the polymerization criterion which is termed the curing voltage. The PSEHD pattern persists after the photopolymerization is completed and the voltage is removed. The EHD instability of GP is sensitive to the applied frequency. As shown in Fig. 3, the conductance regime, characterized by space charge oscillations at lower threshold voltages, is defined in the frequency range of $f < f_c$, where f_c is the critical frequency. When $f > f_c$, the system reaches the dielectric regime, where the period of the electric field is smaller than the relaxation time of space charge and V_{th} varies with $f^{1/2}$ [19].

#243823 Received 25 Jun 2015; revised 6 Aug 2015; accepted 11 Aug 2015; published 19 Aug 2015

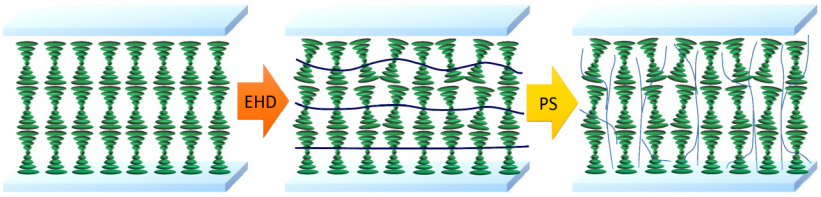

Fig. 1. Schematic of the fabrication of a CLC cell in the initial PSEHD state.

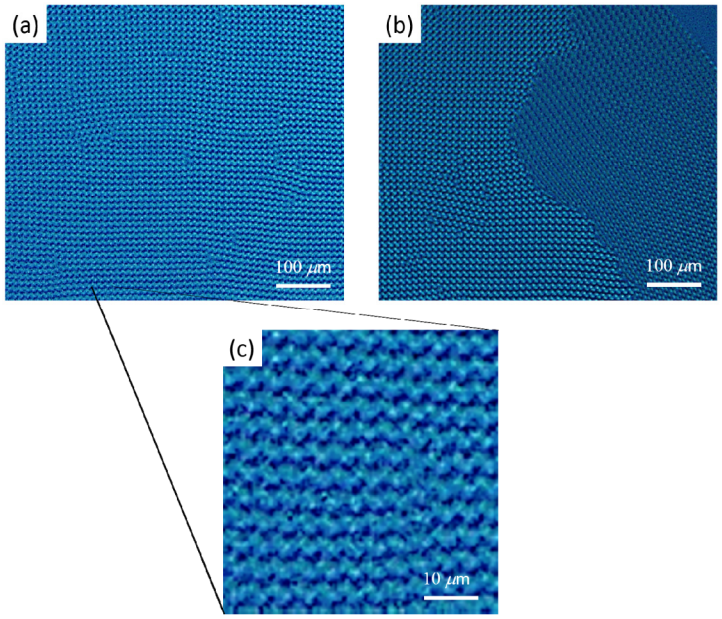

Fig. 2. POM images of (a) a typical EHD GP, (b) a PSEHD GP, and (c) an enlarged (10 ×) size of the EHD GP generated in an initially identical cell containing prepolymer.

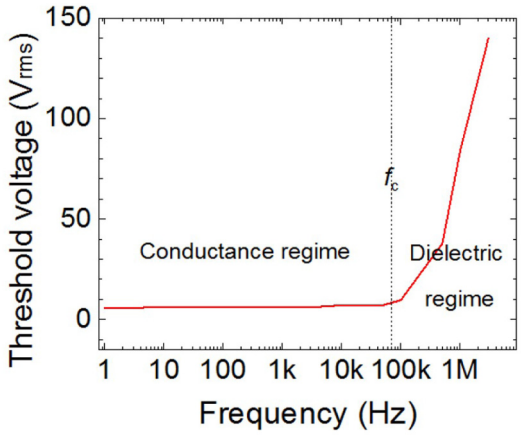

Fig. 3. Frequency-dependent threshold voltage required to induce the GP state. f_c is the critical frequency.

#243823 Received 25 Jun 2015; revised 6 Aug 2015; accepted 11 Aug 2015; published 19 Aug 2015

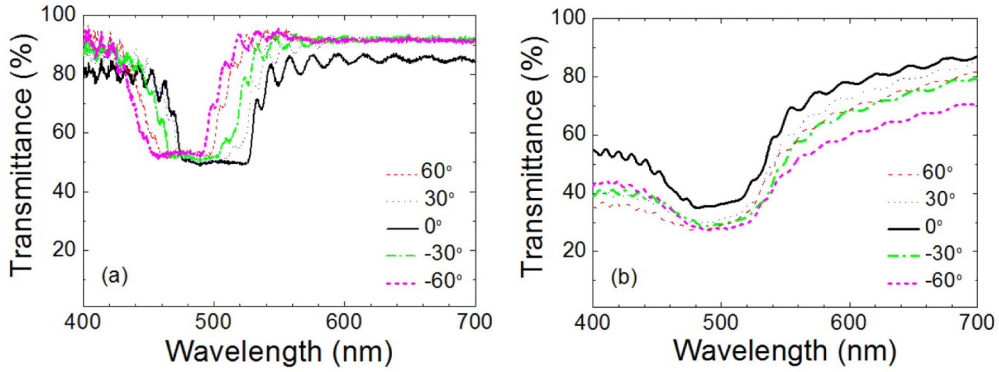

Fig. 4. Comparative transmittance spectra of (a) a planar CLC cell and (b) a PSEHD cell at various viewing angles.

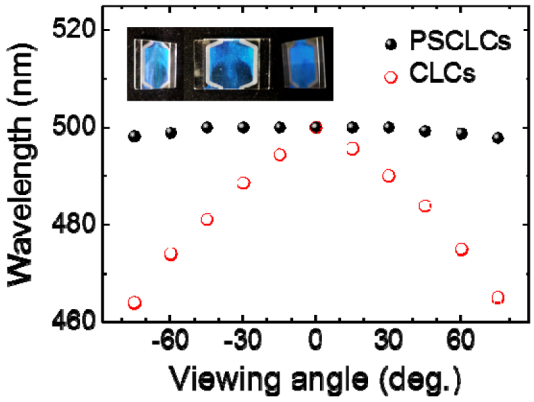

Fig. 5. The central wavelength of the Bragg reflection as a function of the viewing angle. Data are retrieved from Fig. 4. Inset: photographs of a PSEHD cell as viewed at ± 60° (sides) and 0° (middle).

A linearly polarized broadband white-light lamp was used as a source for our measurement of spectra at various viewing angles. Figure 4(a) illustrates the transmission spectra of a planar CLC counterpart (i.e., a conventional CLC cell in the planar state). The angles labeled in the legend are the angles of reflection measured from the normal to the cell plane. For oblique light incidence at an angle θ into a CLC or PSCLC cell, the central wavelength of the Bragg reflection, λ, is proportional to cos θ and the bandwidth at half maximum $\Delta\lambda$ varies linearly with cos θ as well. The reflection intensity reaches a maximum at the Bragg angle and declines rapidly as the angle deviates further from the Bragg angle. It is obvious in Fig. 4(a) that, following Bragg's law, both the central wavelength and the bandwidth at half maximum of the reflection band blueshift in the pristine CLC cell. As a result, the reflected color depends strongly on the viewing angle or the line of sight. This phenomenon, regarded as a drawback, makes conventional CLCs unsuitable for use in displays that demand a wide viewing angle. In comparison with Fig. 4(a), Fig. 4(b) presents the transmittance spectra of a PSEHD cell that is much less dispersive than the neat CLC counterpart because of the gridlike structure in the PSCLC. One can see that the reflection band centered at *ca.* 500 nm does not shift with the viewing angle. Noticeably, the gridlike structure in the PSCLCs is not a perfect planar state, which makes the Bragg reflection less sharp or pronounced. Also as expected, the intrinsic gridlike planar structure somewhat induces light scattering to slight lower the overall transmittance as manifested by Fig. 4(b).

#243823 Received 25 Jun 2015; revised 6 Aug 2015; accepted 11 Aug 2015; published 19 Aug 2015

The viewing zone of the PSEHD sample can easily reach 75° without iridescence as shown in Fig. 5. The photographs of the very PSEHD CLC cell viewed at the slant angles of ± 60° and

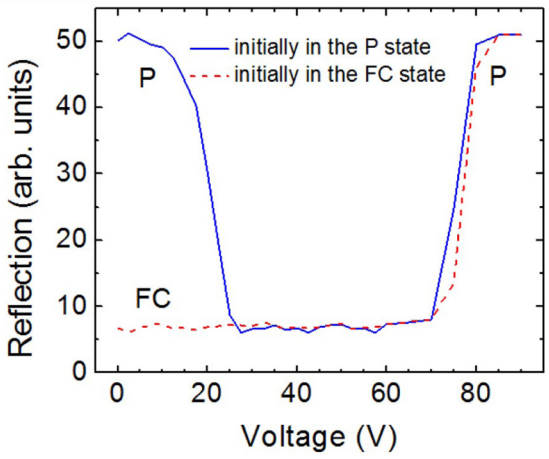

Fig. 6. White-light optical response of a bistable PSEHD CLC cell to voltage pulses of 3 s in pulse width.

in the normal condition (i.e., 0°) are also displayed in Fig. 5 (see the inset). One can see that the view angle is quite wide in the stable PSEHD/CLCs. Compared with conventional CLCs, our method effectively reduces CLC iridescence.

Figure 6 shows the optical response in the visible spectrum of the bistable PSEHD CLC cell upon the agitation by an AC voltage pulse lasting 3 s. The ordinate (i.e., vertical axis) represents the reflectance measured after the removal of the voltage pulse. The solid and dashed curves represent the reflectance of the PSCLC that is initially in the planar and focal conic states, respectively. When the voltage of the pulse is smaller than 22 V_{rms}, the CLC remains in its original state both during and after the voltage pulse. When the voltage is increased beyond 22 V_{rms}, some grid domains are switched into the focal conic state, thereby reducing the reflectance. When the voltage of pulse is increased above 80 V_{rms}, all of the domains are switched to the homeotropic state and the PSCLC relaxes to the planar state after the 3-s pulse ceases, yielding high reflectance. Note that the switching voltage for a PSEHD CLC cell is higher than that for a pristine CLC counterpart. The switching voltage of the pristine CLC in the focal conic state is 18 V_{rms}. When the voltage is increased above 65 V_{rms}, the entire focal conic state is switched to the homeotropic state. Reasonably, the polymer network in the PSEHD cell reduces the effective voltage drop across the LC bulk. Hence, the PSCLC requires a higher voltage to reorient the LC director. In comparison with the literature on widening the viewing angle in CLCs [7,22], this work reveals a simple and feasible approach to fabrication of PSEHD cells that are potentially suitable for applications in non-iridescent optical devices.

4. Conclusions

In summary, a wide viewing angle is particularly important for displays that are intended for use in arbitrary ambient lighting. In this study a grid-patterned multi-domain PSEHD CLC display is demonstrated using a PSEHD film featured by its stabilized GP. A periodic GP is induced by the charge flow and UV irradiation. The helical axis of the PSCLC is aligned normal to the surface of the EHD-GP structure where numerous “protrusions” are present. The GP, clearly observed in the POM images of the PSCLC cell, renders little color shift in reflection and, consequently, results in a wide viewing angle. The PSEHD method is an easy way to achieve non-iridescence of CLCs. However, the perfect Bragg reflection is sacrificed because of the slight scattering by the unique PSEHD structure. The multi-domain PSEHD

#243823 Received 25 Jun 2015; revised 6 Aug 2015; accepted 11 Aug 2015; published 19 Aug 2015

CLC is simple to fabricate and potentially suitable for applications in wide-viewing-angle display and non-iridescent optical devices. It is worth reminding here that many relevant works on bistable properties or measurements of CLC optics have been demonstrated by Kent Displays Incorporated [23] and previously proposed by Yang and associates [8–10].

Acknowledgment

This work was financially supported by the Ministry of Science and Technology, Taiwan, under grant Nos. 103-2923-M-009-003-MY3 and 104-2112-M-009-008-MY3.

#243823 Received 25 Jun 2015; revised 6 Aug 2015; accepted 11 Aug 2015; published 19 Aug 2015